Advances in Radiation Oncology (2021) 7, 100844

advances in radiation oncology

www.advancesradonc.org

Scientific Article

Quantifying Systematic RBE-Weighted Dose Uncertainty Arising from Multiple Variable RBE Models in Organ at Risk

Wei Yang Calvin Koh, BSc,[a,b] Hong Qi Tan, PhD,[b] Yan Yee Ng, MSc,[b] Yen Hwa Lin, PhD,[b] Khong Wei Ang, MSc,[b] Wen Siang Lew, PhD,[a] James Cheow Lei Lee, PhD,[a,b] and Sung Yong Park, PhD[b,c,*]

[a]*Division of Physics and Applied Physics, Nanyang Technological University, Singapore;* [b]*Division of Radiation Oncology, National Cancer Centre Singapore, Singapore;* [c]*Oncology Academic Clinical Programme, Duke-NUS Medical School, National University of Singapore, Singapore*

Received June 12, 2021; revised September 27, 2021; accepted October 29, 2021

Abstract

Purpose: Relative biological effectiveness (RBE) uncertainties have been a concern for treatment planning in proton therapy, particularly for treatment sites that are near organs at risk (OARs). In such a clinical situation, the utilization of variable RBE models is preferred over constant RBE model of 1.1. The problem, however, lies in the exact choice of RBE model, especially when current RBE models are plagued with a host of uncertainties. This paper aims to determine the influence of RBE models on treatment planning, specifically to improve the understanding of the influence of the RBE models with regard to the passing and failing of treatment plans. This can be achieved by studying the RBE-weighted dose uncertainties across RBE models for OARs in cases where the target volume overlaps the OARs. Multi-field optimization (MFO) and single-field optimization (SFO) plans were compared in order to recommend which technique was more effective in eliminating the variations between RBE models.

Methods: Fifteen brain tumor patients were selected based on their profile where their target volume overlaps with both the brain stem and the optic chiasm. In this study, 6 RBE models were analyzed to determine the RBE-weighted dose uncertainties. Both MFO and SFO planning techniques were adopted for the treatment planning of each patient. RBE-weighted dose uncertainties in the OARs are calculated assuming $\left(\frac{\alpha}{\beta}\right)_x$ of 3 Gy and 8 Gy. Statistical analysis was used to ascertain the differences in RBE-weighted dose uncertainties between MFO and SFO planning. Additionally, further investigation of the linear energy transfer (LET) distribution was conducted to determine the relationship between LET distribution and RBE-weighted dose uncertainties.

Results: The results showed no strong indication on which planning technique would be the best for achieving treatment planning constraints. MFO and SFO showed significant differences (P <.05) in the RBE-weighted dose uncertainties in the OAR. In both clinical target volume (CTV)-brain stem and CTV-chiasm overlap region, 10 of 15 patients showed a lower median RBE-weighted dose uncertainty in MFO planning compared with SFO planning. In the LET analysis, 8 patients (optic chiasm) and 13 patients (brain stem) showed a lower mean LET in MFO planning compared with SFO planning. It was also

Sources of support: This work is partially supported by the Duke-NUS Oncology Academic Clinical Programme Proton Research fund (08/FY2019/EX(SL)/65-A111) and Duke-NUS Oncology Academic Clinical Programme Proton Research fund (08/FY2020/EX(SL)/76-A152).

Disclosures: The authors declare that the research was conducted in the absence of any commercial or financial relationships that could be construed as a potential conflict of interest.

Research data are not available at this time.

*Corresponding author: Sung Yong Park, PhD; E-mail: sung.yong.park@nccs.com.sg

https://doi.org/10.1016/j.adro.2021.100844

observed that lesser RBE-weighted dose uncertainties were present with MFO planning compared with SFO planning technique.

Conclusions: Calculations of the RBE-weighted dose uncertainties based on 6 RBE models and 2 different $\left(\frac{\alpha}{\beta}\right)_x$ revealed that MFO planning is a better option as opposed to SFO planning for cases of overlapping brain tumor with OARs in eliminating RBE-weighted dose uncertainties. Incorporation of RBE models failed to dictate the passing or failing of a treatment plan. To eliminate RBE-weighted dose uncertainties in OARs, the MFO planning technique is recommended for brain tumor when CTV and OARs overlap.

Introduction

Proton therapy (PT) has an advantage over conventional radiation therapy for tumors that are located near organs at risk (OARs). This is due to its unique physical interaction resulting in Bragg peak where there is a steep dose fall-off at the distal end of the proton range. Despite the well-known physical properties of a proton beam, biological uncertainties are a concern, that is specifically the relative biological effectiveness (RBE) uncertainties.

Currently, a constant RBE of 1.1 is used clinically to include the differential biological effect of protons compared with photons during treatment planning. It is a conservative estimate based on in vivo RBE experimental results in the spread-out Bragg peak (SOBP). The need for variable RBE models is also eliminated as the effect in RBE at the end of range may be mitigated by range uncertainties.[1]

However, the counterargument against the use of a constant RBE of 1.1 stems from the possibility of underdosing or overdosing in the target volume. As suggested by AAPM TG-256,[1] there is a need to understand the spatial variations of RBE within and outside the target volume on a voxel-wise basis. This can be inferred from the evidence of experiments that showed RBE exceeding 1.1 at the end of range.[2-4] Hence, RBE-weighted dose is especially important when the target volume is extremely close to the OARs.

Numerous variable RBE models have been proposed,[5-10] with the more prominent ones being local effect model (LEM) and microdosimetric kinetic model (MKM). Despite the long history of variable RBE models, the adoption of the variable RBE models has been modest in the clinic due to the large uncertainties in RBE values.[11] These uncertainties arise from uncertainties in alpha-beta ratio $\left(\frac{\alpha}{\beta}\right)_x$ (patient sensitivity), dose-averaged linear energy transfer, cell-lines used in the experiments, and the experimental setup.[12] Apart from the variable RBE model approach, another approach using a combination of dose and LET was also established.[13-18] This approach is motivated by the correlation between LET and RBE, where RBE increases with LET along the proton beam path. Presently, there are no commercial and *clinical* treatment planning systems (TPSs) that can provide LET-guided optimization during treatment planning or calculate variable RBE-weighted dose.

After the TG-256 report, variable RBE models are recommended for certain clinical situations (OARs close to target). However, it does not provide recommendations on the exact RBE models to be used. This provides the motivation for this study, where the dose difference arising from the use of various variable linear quadratic (LQ)-based RBE models was examined. Clinical sites where OARs were situated close to or overlapping the target volume were chosen as these were the clinical cases where variable RBE models would be highly relevant. Multi-field optimization (MFO) or single-field optimization (SFO) treatment planning was then used on these clinical cases.

In SFO planning, the beam spot position and weightage of each field are optimized individually to fulfill the dose coverage, whereas in MFO planning, all beam spots of all fields are optimized simultaneously where different fields can be used to cover different parts of the tumor to achieve a highly conformal dose distribution. Currently, MFO planning is known to yield a better plan quality compared with SFO planning.[19-21] Tommasino et al[21] stated that there were no statistically significant differences in RBE-weighted dose increase between MFO and SFO planning based on McNamara's RBE model.[8] However, Unkelbach et al revealed that MFO planning has a higher RBE-variable dose compared with SFO planning.[14] This could be due to MFO providing more degrees of freedom to allocate higher LET doses within the target. To the best of our knowledge, there is no literature on whether MFO or SFO planning can lead to a model-agnostic RBE dose distribution.

In this study, the area of interest lies in the brain tumor where the clinical target volume (CTV) overlaps with the brain stem (CTV-BS) and optic chiasm (CTV-CH). In these overlapping regions, RBE-weighted dose uncertainties were analyzed based on the 6 RBE models in the overlapping regions (CTV-BS and CTV-CH) and OARs (brain stem and optic chiasm). Different $\left(\frac{\alpha}{\beta}\right)_x$ were also applied to the RBE models. Subsequently, the RBE models were implemented on both MFO and SFO planning to determine whether there was any difference in RBE-weighted dose uncertainties distribution. This enabled the determination of which planning technique (MFO vs

SFO) was more suitable for arriving at an RBE model-agnostic dose distribution.

Methods

Patient characteristics

In this study, 15 retrospective patients with brain tumors of specific features were selected. The types of brain tumors involve in this study are glioblastoma, astrocytoma, and oligodendroglioma. The CTV of each patient overlapped with OARs (brain stem and optic chiasm) as shown in Table E1. All patients were treated with photon radiation therapy treatment before 2017, and the institutional board had approved this study. They were replanned by a trained and experienced dosimetrist (anonymized for review), and all plans were clinically approved for proton therapy treatment.

Treatment planning

The treatment planning criteria used in this study follows the "anonymized for review" protocol, which follows closely to the Radiation Therapy Oncology Group guideline. CTVs were created using a 2-cm uniform expansion from gross tumor volume. Sixty Gy was prescribed over 30 fractions for the tumor used in this study. These plans were optimized to achieve $D_{95} > 60$ Gy, $D_{10} < 63$ Gy and D0.03cc < 63.6 Gy for the CTV. The dose constraint for brain stem and optic chiasm is D0.03cc < 60 Gy.

Each plan consisted of either 2 or 3 proton beams. Gantry angles varied between 0° and 300° for the first beam, 40° and 270° for the second beam, and 90° and 160° for the third beam. The rotation of the couch ranged from 0° to 300°. A range shifter of 4.5 cm water equivalent thickness was used, depending on the distance of the CTV from the skin.

Robust optimization was used on CTV, brain stem, and optic chiasm with 3% range uncertainties and 1 mm setup uncertainties, resulting in a total of 12 scenarios. As the patients are set up using the ExacTrac system (Brainlab AG), less than 1 mm setup uncertainty is expected.

The calculation grid size was set to 0.25 cm and the beam spot full width at half maximum in air was 4.56 mm (228.8 MeV) to 12.7 mm (71.3 MeV) measured at isocenter. Proton convolution superposition algorithm was used to calculate the dose in the treatment planning system (TPS).

Both MFO and SFO techniques followed the same treatment planning protocols. These plans were clinically approved and planned using Eclipse TPS version 15.6 (Varian).

Monte Carlo simulation

All plans were extracted from TPS and recalculated using in-house TOPAS Monte Carlo system (MCS).[22,23] Our in-house TOPAS Monte Carlo dose calculation has been validated against TPS in both water phantom and in patients. The recalculation is necessary because the TPS does not calculate LET and thus the RBE values. The number of particle histories was set to a minimum of 10^7 particles, resulting in a statistical uncertainty in isocenter dose of less than 0.34 %. The physics models used in this study included g4em-standard_opt4, g4h-phy_QGSP_-BERT_HP, g4h-elastic, and g4stopping as these are the recommended physical models for clinical proton beam below 5 GeV.[24] An 80-core Xeon Gold CPU (Intel) running at 2.10 GHz was used for this study. The simulation run time was 4700 protons/s at 150 MeV, and each patient's plan took approximately 2 to 13 hours, depending on the target size. Dose (to medium) and proton LET were saved as DICOM files from the simulation. Nuclear particles are considered in both dose and LET scoring, and the range cut for secondary electron was set to 1 m.

Variable RBE models

In this study, the dose directly obtained from TPS and MCS has been weighted with a constant RBE of 1.1. Six

Table 1 Different LQ-based RBE models used in this study

RBE Models	RBE_{max}	RBE_{min}
Carabe[5]	$0.843 + 0.413644\frac{LET_d}{(\alpha/\beta)_x}$	$1.09 + 0.01612\frac{LET_d}{(\alpha/\beta)_x}$
Chen[6]	$\frac{0.1}{\alpha_x} + \frac{1-e^{-0.0013LET_d^2}}{0.045\alpha_x LET_d}$	1.0
McNamara[8]	$0.99064 + 0.35605\frac{LET_d}{(\alpha/\beta)_x}$	$1.1012 - 0.0039\sqrt{(\alpha/\beta)_x}LET_d$
Wedenberg[10]	$1 + 0.434\frac{LET_d}{(\alpha/\beta)_x}$	1.0
Wilkens[7]	$0.1 + \frac{0.02LET_d}{\alpha_x}$	1.0

Maximum and minimum relative biological effectiveness of each model are shown. All maximum RBEs are dependent on LET_d, whereas the majority of minimum RBEs are independent of LET_d.

Abbreviations: LET_d = linear energy transfer distribution; RBE = relative biological effectiveness; RBE_{max} = maximum relative biological effectiveness; RBE_{min} = minimum relative biological effectiveness.

representative variable RBE models were applied to the physical dose output from MCS to obtain RBE-weighted dose. These variable RBE models are based on the LQ model and are shown in Table 1. $\left(\frac{\alpha}{\beta}\right)_x$ for the brain tumor is set at 3 Gy and 8 Gy to study the variations of RBE-weighted doses under low and high $\left(\frac{\alpha}{\beta}\right)_x$ values.[25] These values are chosen due to the uncertainties in $\left(\frac{\alpha}{\beta}\right)_x$, as shown in the review by van Leeuwen et al.[25]

Statistical analysis

A voxel-wise calculation of RBE-weighted dose standard deviation (SD) is calculated from the 6 RBE models, thus obtaining a spatial RBE-weighted dose SD map for each planning technique and each patient. Statistical analysis was performed on the overlapping region for both $\left(\frac{\alpha}{\beta}\right)_x$ values in CTV-BS and CTV-CH as these were the regions having high RBE-weighted doses while trying to satisfy the dose coverage for CTV. Kruskal-Wallis H-test was first used to test for the significant difference in the RBE-weighted dose SD between the 2 planning techniques across all patients. A post hoc test was then used to determine significant differences of RBE-weighted dose SD between the MFO and SFO planning techniques of each patient. Bonferroni correction was applied for multiple comparison. A 2-sided P value <.05 was considered significant. The aforementioned statistical tests were repeated for the LET distribution for both planning techniques across all patients and within each patient.

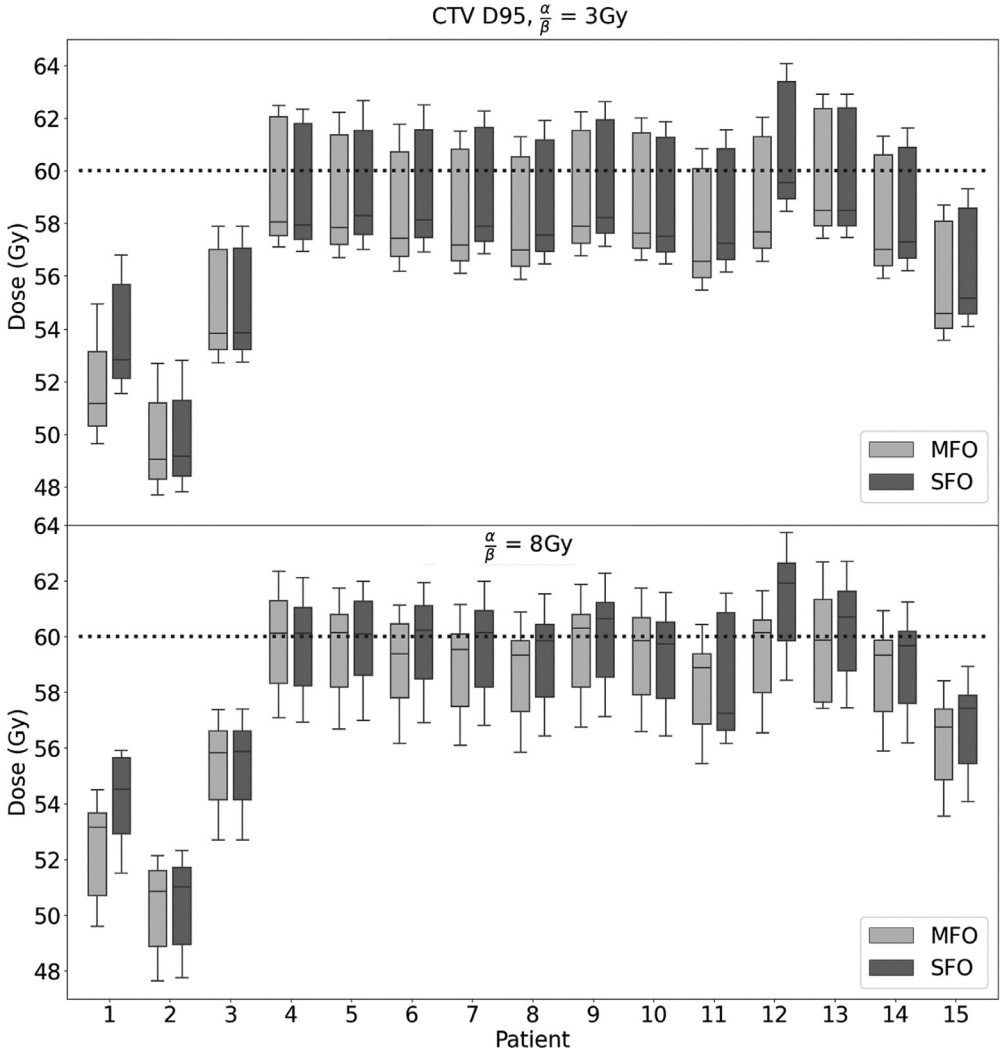

Figure 1 CTV D_{95} of both $\left(\frac{\alpha}{\beta}\right)_x$. Six RBE models were applied to both MFO and SFO planning. Δ/◯ shows the dose of each RBE model. The green Δ/◯ represents RBE 1.1. The dotted line refers to the dose prescribed to the tumor. *Abbreviations*: CTV = clinical target volume; MFO = multi-field optimization; RBE = relative biological effectiveness; SFO = single-field optimization.

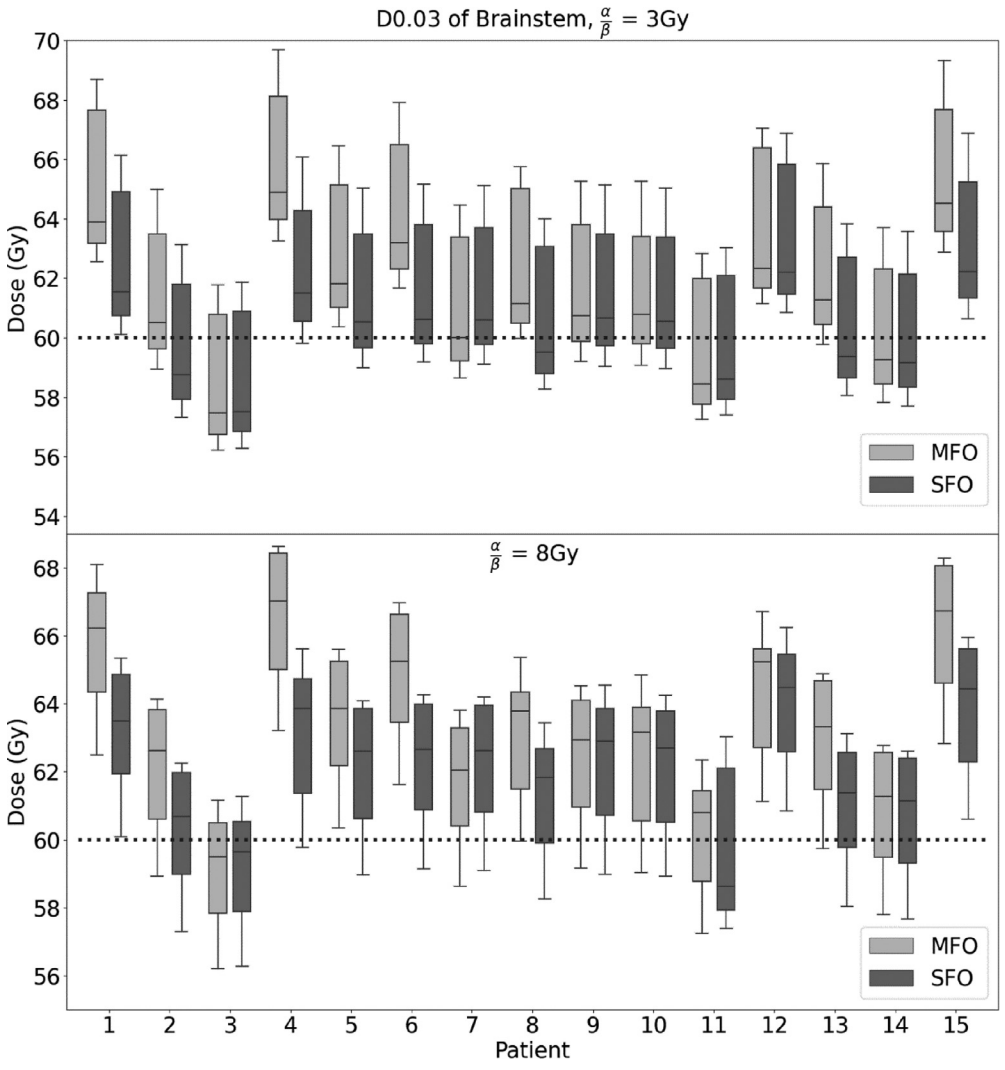

Figure 2 D0.03cc of brain stem for both $\left(\frac{\alpha}{\beta}\right)_x$. Six RBE models were applied to both MFO and SFO planning. Δ/◯ shows the dose of each RBE models. The green Δ/◯ represents RBE 1.1. The dotted line refers to the tumor dose constraint of 60 Gy. *Abbreviations*: MFO = multi-field optimization; RBE = relative biological effectiveness; SFO = single-field optimization.

Results

CTV coverage and OARs dose constraint

Figure E1 shows the dose distribution of a patient for MFO and SFO planning. There were no distinct visual differences in conformality. For all patients, target coverage in TPS was similar where it fulfilled the criteria for D_{95}. D_{10} for CTV and D0.03cc for both CTV and OARs were within constraints. Figures 1, 2, and E2 show the boxplot of CTV D_{95}, brain stem D0.03cc and optic chiasm D0.03cc, respectively. These were calculated for all patients based on RBE 1.1, and the RBE models with different $\left(\frac{\alpha}{\beta}\right)_x$. Assuming a $\left(\frac{\alpha}{\beta}\right)_x$ of 8 Gy led to an increase in median RBE-weighted dose for CTV D_{95} and OAR D0.03cc compared with $\left(\frac{\alpha}{\beta}\right)_x$ of 3 Gy.

In Figure 1, SFO planning technique is observed to have a slight edge over MFO in terms of CTV coverage. The difference between the median RBE-weighted dose and 60 Gy is lesser for SFO compared with MFO. In Figures 2 and E2, the difference between median dose of D0.03cc and 60 Gy (dose constraint) is lesser for both OARs in SFO compared with MFO plans.

Dose uncertainties in CTV-OAR overlapping regions

Figures 3 and E4 show the violin plot of the RBE-weighted dose SD in the overlapping region between CTV-BS and CTV-CH with different $\left(\frac{\alpha}{\beta}\right)_x$ values, respectively. In the CTV-BS overlap region, 10 of 15 patients

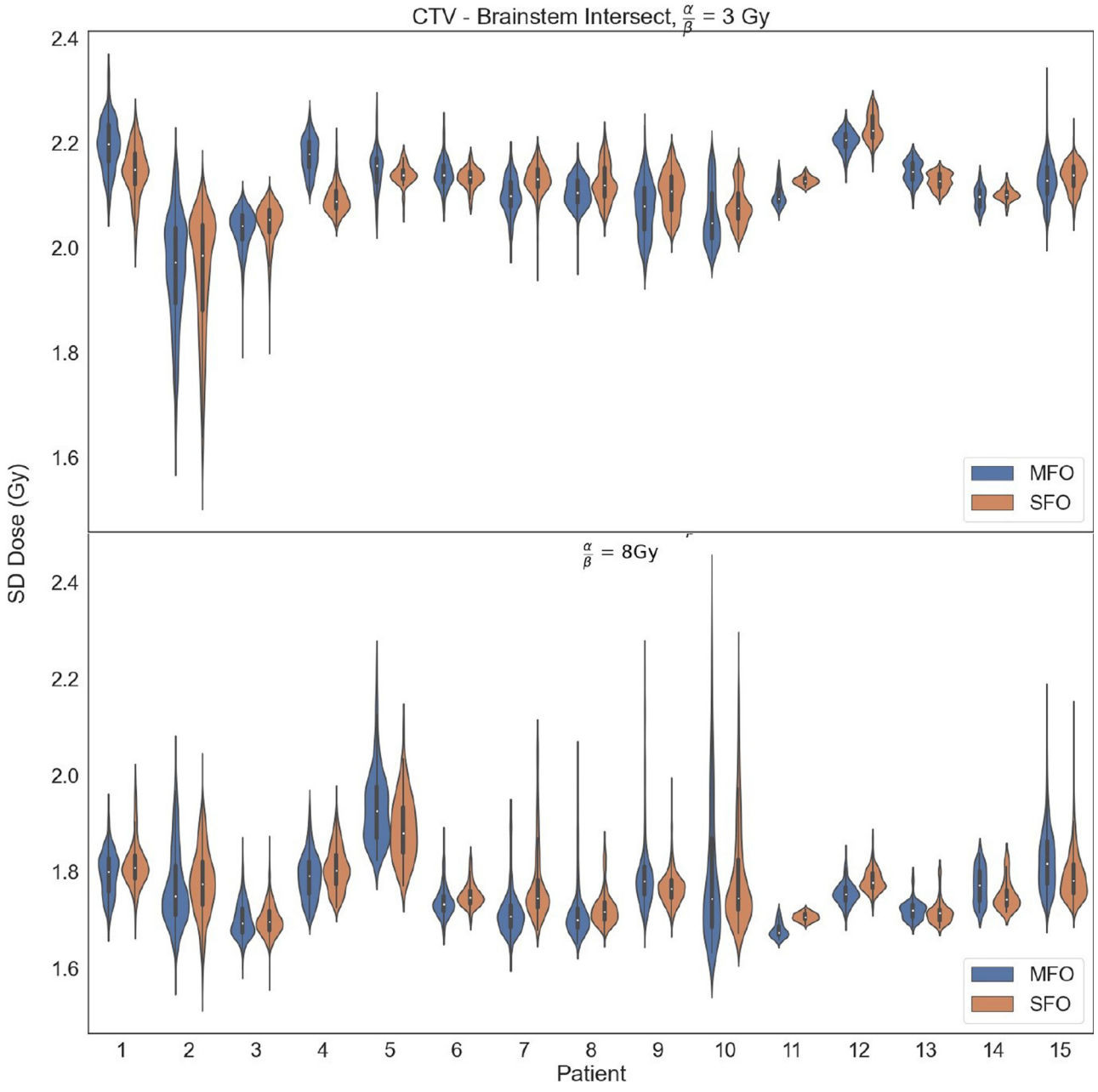

Figure 3 Violin plot of RBE-weighted dose uncertainties based on the 6 RBE models in the CTV-brain stem intersecting regions for both $\left(\frac{\alpha}{\beta}\right)_x$. *Abbreviations*: CTV = clinical target volume; MFO = multi-field optimization; RBE = relative biological effectiveness; SD = standard deviation; SFO = single-field optimization.

have lower median RBE-weighted dose SD when using MFO planning compared with SFO planning. The median RBE-weighted dose SD ranges from 1.6 to 1.9 Gy for high $\left(\frac{\alpha}{\beta}\right)_x$ and 1.9 to 2.2 Gy for low $\left(\frac{\alpha}{\beta}\right)_x$. CTV-CH follows a similar trend as CTV-BS, where 10 of 15 patients have lower median RBE-weighted dose SD in MFO planning compared with SFO planning. The median RBE-weighted dose SD ranges from 1.5 to 2 Gy for high $\left(\frac{\alpha}{\beta}\right)_x$ and 1.5 to 2.2 Gy for low $\left(\frac{\alpha}{\beta}\right)_x$. There is a statistically significant difference (P <.01) between MFO and SFO planning in terms of RBE-weighted dose SD.

LET in OARs

Figure E5 shows the LET distribution in the axial plane between MFO and SFO planning of a patient where the beam angles are set at 290° and 180°. Figure 4 shows the LET distribution difference between MFO and SFO planning in the overlapping region of CTV and OARs (brain stem and optic chiasm). Figure 5 shows the voxel-wise plot of LET distribution against RBE-weighted dose SD $[\alpha\beta x = 8\ Gy]$ map of the same patient's CTV, OARs, and the intersecting region between CTV and OARs for MFO

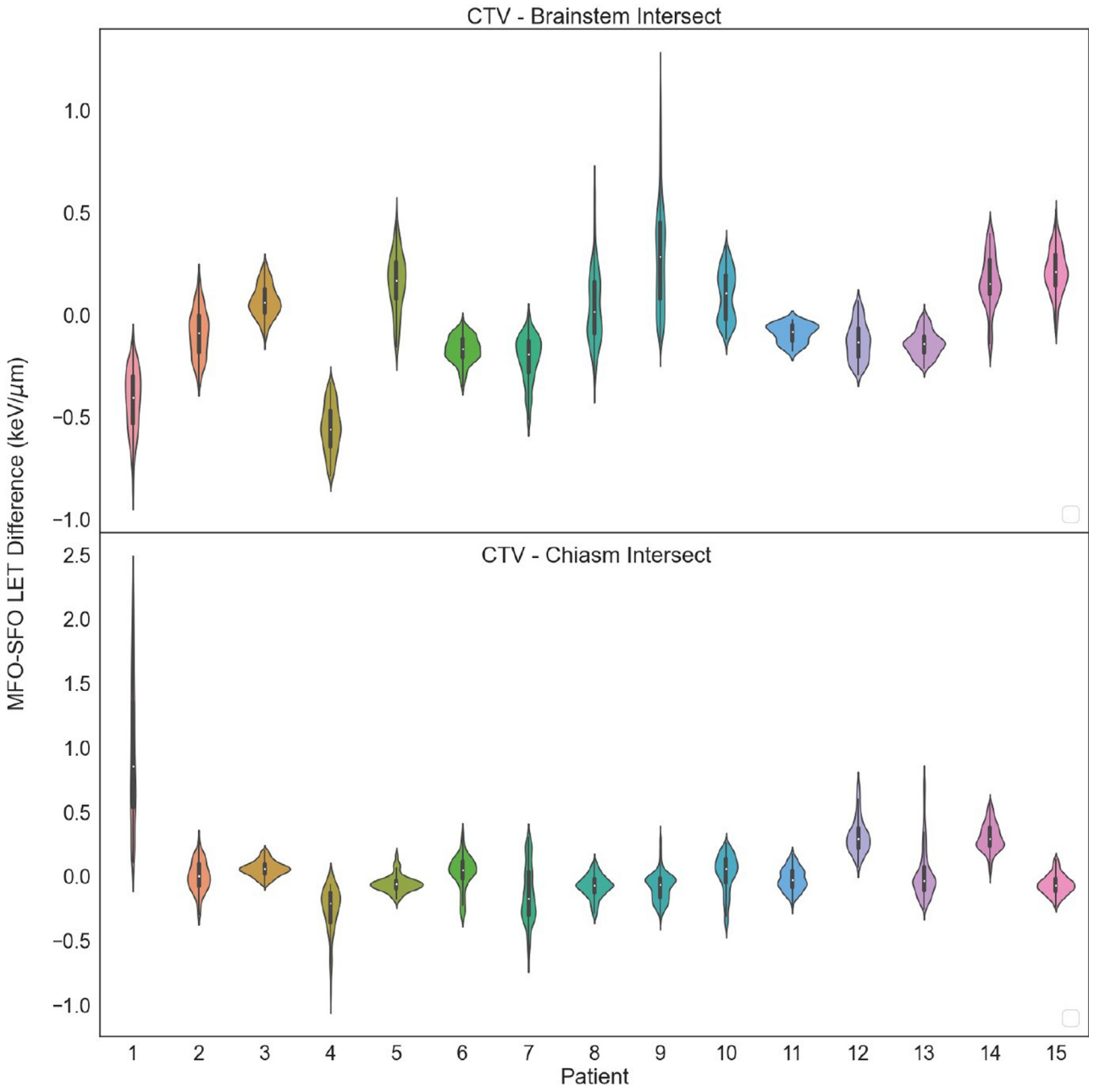

Figure 4 Difference in LET distribution between MFO and SFO plan of each patient in the CTV-brain stem and CTV-chiasm intersecting regions. These data were obtained from Figures E6 and E7, which show the LET distribution of MFO and SFO individually. *Abbreviations*: CTV = clinical target volume; LET = linear energy transfer; MFO = multi-field optimization; SFO = single-field optimization.

and SFO plan. In the CTV and the intersecting region of CTV and OARs, RBE-weighted dose SD increases with increasing LET for both MFO and SFO plan. Figure E9 (A) and (B) shows the voxel-wise kernel density plot of LET distribution against RBE-weighted dose SD [$\alpha\beta x = 8\ Gy$] map of the patient for MFO and SFO plan of a patient. The low LET region ($2-6\ keV/\mu m$) corresponding to RBE-weighted dose SD ($<0.125\ Gy$) is heavily weighted for both MFO and SFO plan. The kernel island at higher RBE-weighted dose SD ($1.5-2.5\ Gy$) corresponds to the high LET in the intersecting region between CTV and OARs, as shown in Figure 5.

There is no clear trend on which planning technique results in a higher LET distribution. In the nonoverlapping region of OARs, lower median LET in MFO planning was observed compared with SFO planning for optic chiasm (8 patients) and brain stem (13 patients).

Figure E8 shows the voxel-wise difference in LET between MFO and SFO planning for both brain stem and optic chiasm. In the entire brain stem, 14 patients have a

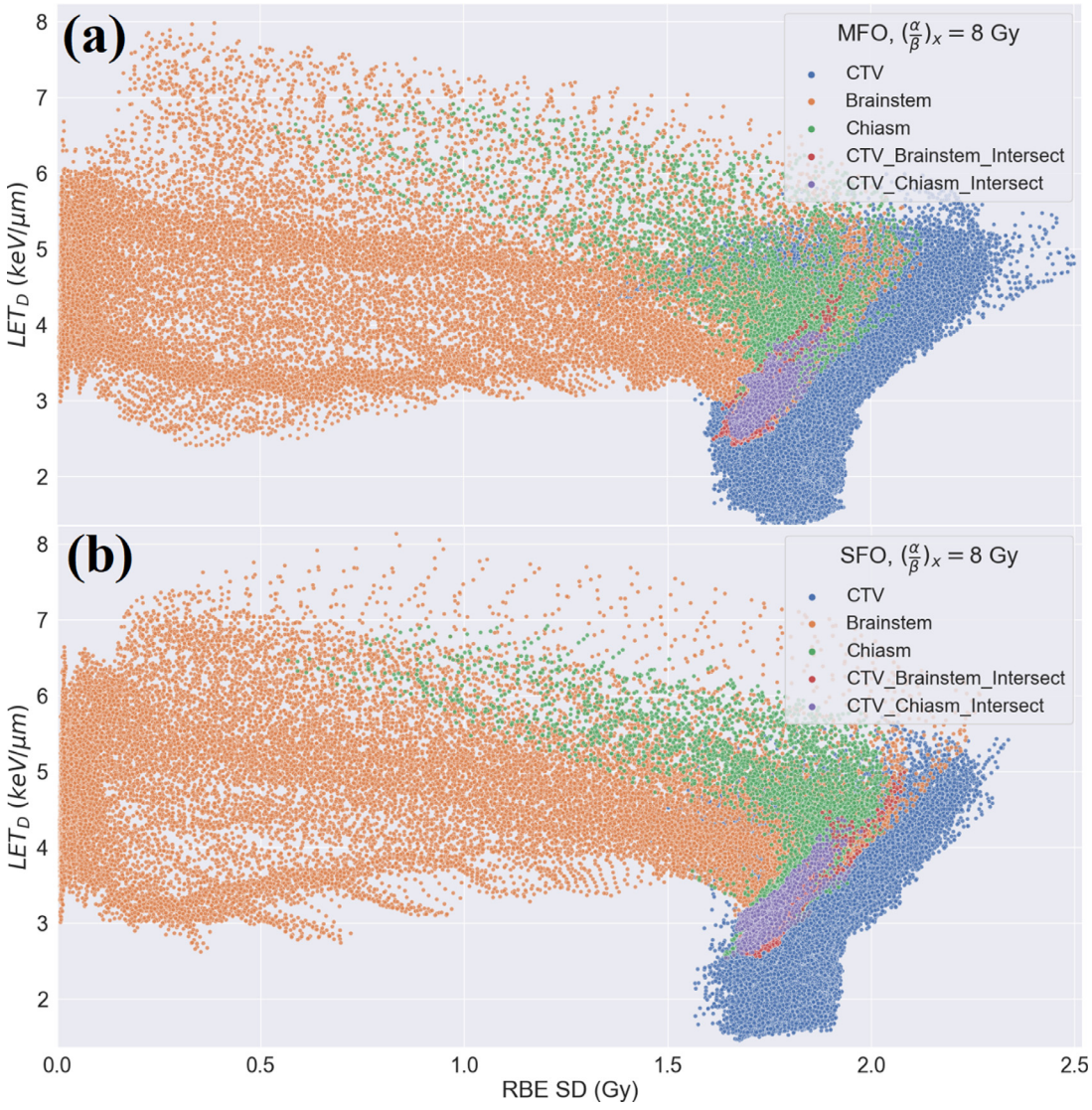

Figure 5 (a) and (b) show the voxel-wise plot of LET_D vs relative biological effectiveness-weighted dose standard deviation of the CTV, organs at risk, and the intersecting regions of CTV and organs at risk for MFO and SFO plan of the same patient respectively. $\left(\frac{\alpha}{\beta}\right)_x = 8\ Gy$ is used in these plots. *Abbreviations:* CTV = clinical target volume; LET_D = linear energy transfer distribution; MFO = multi-field optimization; SFO = single-field optimization.

lower mean LET in MFO planning compared with SFO planning; in the entire optic chiasm, 9 patients have lower mean LET in MFO planning compared with SFO planning. The majority of MFO planned patients showed lower LET values compared with SFO planned patients in this study.

Discussion

In RBE modeling, LQ based models are either using empirical data from clonogenic cell survival for curve fitting or mechanistic hypotheses of radiation action such MKM[26,27] and LEM[28] models. However, only empirical LQ-based RBE models are used in this study. Many studies have been done on the comparison between the different RBE models,[9,29-31] and the novelty of our work lies in achieving a model agnostic in RBE-weighted dose distribution with 2 different treatment planning techniques.

MFO and SFO planning was performed in 15 patients to study the RBE-weighted dose differences in the OAR resulting from 6 representative variable LQ-based RBE models (including the constant 1.1 RBE model). MFO planning shows a better target coverage[19-21] compared with SFO planning. In this study, all RBE models and

RBE 1.1 are compared. Looking at the RBE 1.1 data points alone, the majority of the patients exhibited better target coverage with MFO planning compared with SFO planning. Nonetheless, SFO planning has a slight advantage over MFO planning in relation to dose coverage. This is due to the smaller difference between the median RBE-weighted dose and 60 Gy at D_{95} for both high and low $\left(\frac{\alpha}{\beta}\right)_x$ when all RBE models are considered. Based on the RBE formalism, an increase in $\left(\frac{\alpha}{\beta}\right)_x$ value (Gy) will lead to an increase in RBE-weighted dose, as shown in Figure 1. Regardless of the change in LET distribution (MFO/SFO planning) and $\left(\frac{\alpha}{\beta}\right)_x$ values, comparing D_{95} of CTV and D0.03cc of OARs, Rovik's and Wedenberg's model gave the lowest dose (lower quartile of boxplot) for all patients, whereas Carabe's model gave the highest dose to the majority of the patients. When $\left(\frac{\alpha}{\beta}\right)_x$ increases, the median dose in both D_{95} of CTV and D0.03cc of OARs varies from Chen's (dose increases above median) to Wilkens's or McNamara's model. This trend is similar to the change from SFO to MFO plans, thus showing these models may be more sensitive to LET_D and $\left(\frac{\alpha}{\beta}\right)_x$ change. Additionally, SFO plans have a lower median D0.03cc for both brain stem and optic chiasm as shown in Figures 2 and E2, thus revealing better control of hotspot in the OARs. Overall, it is inconclusive which planning technique would be better for the plan to achieve the dose constraint with the inclusion of RBE models.

The largest contribution of uncertainty to proton therapy lies in the range uncertainty. Many works regarding the range uncertainties in proton therapy have been done, especially in the area of MFO and SFO.[21,32,33] In addition to range uncertainty, RBE-weighted dose is also a concern. As shown by Carabe et al,[34] the biological dose uncertainties will translate to a displacement of the distal end of the RBE-weighted SOBP curve. Considering the overlap between the OARs and CTV, an increase in RBE might lead to a larger depth of the SOBP curve. Thus, it is important to consider the RBE-weighted dose uncertainties between models in the event where the end of range of proton beam might fall in the OARs. The first observation in the result is the distinct difference in RBE-weighted dose SD, where low $\left(\frac{\alpha}{\beta}\right)_x$ leads to higher median RBE-weighted dose SD compared with high $\left(\frac{\alpha}{\beta}\right)_x$ in the OARs. This can be explained by the RBE formalism. When $\left(\frac{\alpha}{\beta}\right)_x$ increases, the RBE-weighted dose decreases for 4 of the RBE models, while the models by Chen[6] and Wilkens[7] return an increase in RBE-weighted dose, assuming a constant α_x and LET. Thus, this reduces the RBE-weighted dose SD in the OARs. Similarly, Marteinsdottir et al[35] had also demonstrated that the impact of a variable RBE is larger in low $\left(\frac{\alpha}{\beta}\right)_x$ compared with high $\left(\frac{\alpha}{\beta}\right)_x$. Therefore, it is advised to be cautious during treatment planning for low $\left(\frac{\alpha}{\beta}\right)_x$ CTV overlaps with OARs.

In the overlapping region between CTV and brain stem, 5 patients had higher median RBE-weighted dose SD in MFO planning compared with SFO planning regardless of $\left(\frac{\alpha}{\beta}\right)_x$. Similarly, in the overlapping region between CTV and chiasm, 4 patients with low $\left(\frac{\alpha}{\beta}\right)_x$ and 5 patients with high $\left(\frac{\alpha}{\beta}\right)_x$ had a higher median RBE-weighted dose SD in MFO planning compared with SFO. There was a significant difference (P <.01) in RBE-weighted dose SD between SFO and MFO for all patients. Comparing the kurtosis and skewness of the RBE-weighted dose SD distribution in these regions for each patient, there was no significant difference between MFO and SFO planning. However, 12 to 14 patients had RBE-weighted dose SD negatively skewed when assuming a higher $\left(\frac{\alpha}{\beta}\right)_x$ in both overlapping regions. From the above results, MFO plans showed lower RBE-weighted dose SD distribution. Hence, there is a higher probability of having lesser RBE-weighted dose uncertainties when RBE models are considered during dose calculation. Therefore, MFO planning can be a better choice in eliminating RBE-weighted dose variations in patients. In other works, MFO plans have also been shown to be superior to SFO plans in terms of plan quality and dose sparing in OAR.[19,21] This supplements the fact that MFO planning might be a better choice in the situation where CTV and OAR overlap.

The LET distribution of each plan is further studied to examine any LET difference between MFO and SFO plans, along with the analytical insights of the uncertainties in the RBE models. As seen in Figure E5, there is no visually detectable difference in LET distribution of the patients between the 2 techniques. Figure 4 shows that more patients possess lower median LET values in the intersecting region between CTV and OAR by MFO planning compared with SFO planning. There is a significant difference (P <.05) in LET distribution between SFO and MFO across all patients for brain stem and optic chiasm. Having a significant difference in LET distribution (P <.05) and RBE-weighted dose SD distribution (P <.01) between MFO and SFO plans further emphasize that there is a significant difference in the dose distribution between MFO and SFO planning technique. The LET distributions in the OARs and overlapping regions are more inhomogeneous and have a higher maximum LET as compare to the CTV in SFO plans, and this is consistent with the findings from Hahn et al.[33] In addition, having higher LET might lead to an increase in RBE-weighted dose and range uncertainties. This is explained by Figure 5, where the CTV and the intersecting regions between CTV and OARs represented by blue, red, and purple markers show the LET increases with RBE-weighted dose SD. Therefore, it will be advantageous to choose MFO plans where the max LET is lower. Considering the results for the entire brain stem and chiasm in Figure E8, MFO planning results were observed to have a lower median LET in the OAR compared with SFO planning. A lower median LET leads to a decrease in RBE dose SD at high $\left(\frac{\alpha}{\beta}\right)_x$ but an increase in RBE-weighted dose SD at low $\left(\frac{\alpha}{\beta}\right)_x$. These LET results are analogous to the analytical analysis of RBE-weighted dose uncertainty across all 6 RBE models as shown in Figure E10. As all the RBE models are

analytical as a function of dose, LET, and $\left(\frac{\alpha}{\beta}\right)_x$, the uncertainties of the RBE models are obtained analytically with these 3 parameters. For the clinical plans, the dose distribution is similar between MFO and SFO planning techniques, $\left(\frac{\alpha}{\beta}\right)_x$ is fixed at $_3\ Gy$ and $_8\ Gy$, and the uncertainty will only be related to the LET distribution. Figure E10 shows the RBE weighted dose SD heat map for both $\left(\frac{\alpha}{\beta}\right)_x$ for a range of LET $_{(0.1-10}\ keV/\mu m)$ and dose $_{(0.1-10}\ Gy)$. It shows an increase in LET will increase the RBE-weighted dose uncertainty. As MFO may have more freedom of redistributing LET, our results show lower median LET values in the OAR of MFO plans compared with SFO plans. This reiterates the higher RBE-weighted dose uncertainty in SFO plans and further explains why the MFO techniques are more effective in reducing RBE-weighted dose uncertainty arising from different RBE models.

LEM and MKM models were not used, which limits the study to only LQ-based RBE models. Further analysis can be done by factoring LEM and MKM models in, to obtain the RBE-weighted dose uncertainties. This methodology can easily be extended to other clinical sites to determine which planning technique is better at reducing RBE-weighted dose uncertainties arising from different RBE models when the OARs are situated close to or overlapping the CTV. In addition, LET optimization can be considered because it has proven to be able to redistribute high LET out of OARs into CTV.[15,18,36] A reduced LET in the OARs will lead to a decrease in RBE-weighted dose uncertainties, as shown in the results. RBE-weighted dose uncertainties can then be examined in the OAR between MFO and SFO planning to determine whether there are any differences in the application of these 2 techniques.

Conclusions

There is no indication of which planning technique would be better in achieving the planning constraint of the brain tumor. In situations in which OARs are extremely close to or overlap the target volume, the results present the case that there is lesser RBE-weighted dose SD in the region of overlap in MFO planning. The median LET in the OAR is lower in most patients using MFO planning compared with using SFO planning. Therefore, MFO is the preferred technique for reducing RBE-weighted dose uncertainties that arise from RBE models, and this is important for OARs near target volume during treatment planning.

Supplementary Materials

Supplementary material associated with this article can be found in the online version at doi:10.1016/j.adro.2021.100844.

References

1. Paganetti H, Blakely E, Carabe-Fernandez A, et al. Report of the AAPM TG-256 on the relative biological effectiveness of proton beams in radiation therapy. *Med Phys*. 2019;46:e53–e78.
2. Matsumoto Y, Matsuura T, Wada M, et al. Enhanced radiobiological effects at the distal end of a clinical proton beam: In vitro study. *J Radiat Res*. 2014;55:816–822.
3. Sørensen BS, Bassler N, Nielsen S, et al. Relative biological effectiveness (RBE) and distal edge effects of proton radiation on early damage in vivo. *Acta Oncol*. 2017;56:1387–1391.
4. Ilicic K, Combs SE, Schmid TE. New insights in the relative radiobiological effectiveness of proton irradiation. *Radiat Oncol*. 2018;13:4–11.
5. Carabe-Fernandez A, Moteabbed M, Depauw N, et al. SU-E-T-648: Range uncertainty in proton therapy due to variable biological effectiveness. *Med Phys*. 2011;38:3639.
6. Chen Y, Ahmad S. Empirical model estimation of relative biological effectiveness for proton beam therapy. *Radiat Prot Dosimetry*. 2012;149:116–123.
7. Wilkens JJ, Oelfke U. A phenomenological model for the relative biological effectiveness in therapeutic proton beams. *Phys Med Biol*. 2004;49:2811–2825.
8. McNamara AL, Schuemann J, Paganetti H. A phenomenological relative biological effectiveness (RBE) model for proton therapy based on all published in vitro cell survival data. *Phys Med Biol*. 2015;60:8399–8416.
9. Rørvik E, Thornqvist S, Stokkevag CH, et al. A phenomenological biological dose model for proton therapy based on linear energy transfer spectra. *Med Phys*. 2017;44:2586–2594.
10. Wedenberg M, Lind BK, Hårdemark B. A model for the relative biological effectiveness of protons: The tissue specific parameter α/β of photons is a predictor for the sensitivity to LET changes. *Acta Oncol*. 2013;52:580–588.
11. Paganetti H. Relating proton treatments to photon treatments via the relative biological effectiveness—should we revise current clinical practice? *Int J Radiat Oncol Biol Phys*. 2015;91:892–894.
12. Tan HQ, Koh WYC, Tan LKR, et al. Dependence of LET on material and its impact on current RBE model. *Phys Med Biol*. 2019;64:135022.
13. Drosoula Giantsoudi PD, Clemens Grassberger M, David Craft PD, et al. Linear energy transfer (LET)-guided optimization in intensity modulated proton therapy (IMPT): Feasibility study and clinical potential. *Int J Radiat Oncol Biol Phys*. 2015;73:389–400.
14. Unkelbach J, Botas P, Giantsoudi D, Gorissen BL, Paganetti H. Reoptimization of intensity modulated proton therapy plans based on linear energy transfer. *Int J Radiat Oncol Biol Phys*. 2016;96:1097–1106.
15. Cao W, Khabazian A, Yepes P, et al. Reply to comment on "Linear energy transfer incorporated intensity modulated proton therapy optimization. *Phys Med Biol*. 2019;64: 058002.
16. Fjæra LF, Li Z, Ytre-Hauge KS, et al. Linear energy transfer distributions in the brainstem depending on tumour location in intensity-modulated proton therapy of paediatric cancer. *Acta Oncol*. 2017;56:763–768.
17. Toussaint L, Indelicato DJ, Holgersen KS, et al. Towards proton arc therapy: Physical and biologically equivalent doses with increasing number of beams in pediatric brain irradiation. *Acta Oncol*. 2019;58:1451–1456.
18. Liu C, Patel SH, Shan J, et al. Robust optimization for intensity modulated proton therapy to redistribute high linear energy transfer from nearby critical organs to tumors in head and neck cancer. *Int J Radiat Oncol Biol Phys*. 2020;107:181–193.
19. Quan EM, Liu W, Wu R, et al. Preliminary evaluation of multifield and single-field optimization for the treatment planning of spot-scanning proton therapy of head and neck cancer. *Med Phys*. 2013;40: 081709.

20. Barten DLJ, Tol JP, Dahele M, Slotman BJ, Verbakel WFAR. Comparison of organ-at-risk sparing and plan robustness for spot-scanning proton therapy and volumetric modulated arc photon therapy in head-and-neck cancer. *Med Phys*. 2015;42:6589–6598.
21. Tommasino F, Widesott L, Fracchiolla F, et al. Clinical implementation in proton therapy of multi-field optimization by a hybrid method combining conventional PTV with robust optimization. *Phys Med Biol*. 2020;65: 045002.
22. Perl J, Shin J, Schümann J, et al. TOPAS: An innovative proton Monte Carlo platform for research and clinical applications. *Med Phys*. 2012;39:6818–6837.
23. Faddegon B, Ramos-Méndez J, Schuemann J, et al. The TOPAS tool for particle simulation, a Monte Carlo simulation tool for physics, biology and clinical research. *Phys Med*. 2020;72:114–121.
24. Guan F, Peeler C, Bronk L, et al. Analysis of the track- and dose-averaged LET and LET spectra in proton therapy using the geant 4 Monte Carlo code. *Med Phys*. 2015;42:6234–6247.
25. van Leeuwen CM, Oei AL, Crezee J, et al. The alfa and beta of tumours: A review of parameters of the linear-quadratic model, derived from clinical radiotherapy studies. *Radiat Oncol*. 2018;13:1–11.
26. Inaniwa T, Furukawa T, Kase Y, et al. Treatment planning for a scanned carbon beam with a modified microdosimetric kinetic model. *Phys Med Biol*. 2010;55:6721–6737.
27. Kamada T, Tsujii H, Blakely EA, et al. Carbon ion radiotherapy in Japan: An assessment of 20 years of clinical experience. *Lancet Oncol*. 2015;16:e93–e100.
28. Scholz M, Kellerer AM, Kraft-Weyrather W, et al. Computation of cell survival in heavy ion beams for therapy. *Radiat Environ Biophys*. 1997;36:59–66.
29. McNamara AL, Schuemann J, Paganetti H. A phenomenological relative biological effectiveness (RBE) model for proton therapy based on all published in vitro cell survival data. *Phys Med Biol*. 2015;60:8399.
30. Giovannini G, Böhlen T, Cabal G, et al. Variable RBE in proton therapy: Comparison of different model predictions and their influence on clinical-like scenarios. *Radiat Oncol*. 2016;11:1–16.
31. McNamara A, Willers H, Paganetti H. Proton Therapy special feature: Review article modelling variable proton relative biological effectiveness for treatment planning. *Br J Radiol*. 2019;92: 20190334.
32. Cubillos-Mesías M, Baumann M, Troost EGC, et al. Impact of robust treatment planning on single- and multi-field optimized plans for proton beam therapy of unilateral head and neck target volumes. *Radiat Oncol*. 2017;12:1–10.
33. Hahn C, Eulitz J, Peters N, et al. Impact of range uncertainty on clinical distributions of linear energy transfer and biological effectiveness in proton therapy. *Med Phys*. 2020;47:6151–6162.
34. Carabe A, Moteabbed M, Depauw N, et al. Range uncertainty in proton therapy due to variable biological effectiveness. *Phys Med Biol*. 2012;57:1159.
35. Marteinsdottir M, Schuemann J, Paganetti H. Impact of uncertainties in range and RBE on small field proton therapy. *Phys Med Biol*. 2019;64:1–10.
36. Giantsoudi D, Grassberger C, Craft D, et al. Linear energy transfer-guided optimization in intensity modulated proton therapy: Feasibility study and clinical potential. *Int J Radiat Oncol Biol Phys*. 2013;87:216–222.